



Ultrafiltration technology with a ceramic membrane for reactive dye removal: Optimization of membrane performance

E. Alventosa-deLara*, S. Barredo-Damas, M.I. Alcaina-Miranda, M.I. Iborra-Clar

Department of Chemical and Nuclear Engineering, Universitat Politècnica de València, Camino de Vera s/n, 46022 Valencia, Spain

ARTICLE INFO

Article history:

Received 15 August 2011

Received in revised form

28 November 2011

Accepted 19 January 2012

Available online 28 January 2012

Keywords:

Ultrafiltration

Ceramic membrane

Reactive dye

Response surface methodology

Optimization

ABSTRACT

An ultrafiltration (UF) ceramic membrane was used to decolorize Reactive Black 5 (RB5) solutions at different dye concentrations (50 and 500 mg/L). Transmembrane pressure (TMP) and cross-flow velocity (CFV) were modified to study their influence on initial and steady-state permeate flux (J_p) and dye rejection (R). Generally, J_p increased with higher TMP and CFV and lower feed concentration, up to a maximum steady-state J_p of 266.81 L/(m² h), obtained at 3 bar, 3 m/s and 50 mg/L. However, there was a TMP value (which changed depending on operating CFV and concentration) beyond which slight or no further increase in steady-state J_p was observed. Similarly, the higher the CFV was, the more slightly the steady-state J_p increased. Furthermore, the effectiveness of ultrafiltration treatment was evaluated through dye rejection coefficient. The results showed significant dye removals, regardless of the tested conditions, with steady-state R higher than 79.8% for the 50 mg/L runs and around 73.2% for the 500 mg/L runs.

Finally response surface methodology (RSM) was used to optimize membrane performance. At 50 mg/L, a TMP of 4 bar and a CFV of 2.53 m/s were found to be the conditions giving the highest steady-state J_p , 255.86 L/(m² h), and the highest R , 95.2% simultaneously.

© 2012 Elsevier B.V. All rights reserved.

1. Introduction

Textile dyeing is among the most environmentally unfriendly industrial processes owing to the large quantities of water demanded and the strongly colored wastewater produced, polluted with dyes and other chemical auxiliaries. Azo reactive dyes, as Reactive Black 5 (RB5), are widely used in dyeing processes since they present unique properties and technical characteristics [1]. Unfortunately, the use of this class of dyes has also undesirable consequences from the ecological point of view. Poor dye-fiber fixation has been a long-standing problem with reactive dyes and as a result, between 20 and 50% of the applied reactive dye is discharged in wastewater effluent [2]. The first noticeable effect in the receiving water is the color, which not only causes aesthetic impact, but can also interrupt photosynthesis, thus affecting aquatic life [3]. Other effects are related to dye degradation products, including aromatic amines, which are known to be toxic and potentially carcinogenic [4]. Therefore, these wastewaters must be adequately treated before disposal.

Biological treatment [5], adsorption onto activated carbon [6] or other adsorbents [7], and other non-conventional technologies

such as electrocoagulation [8] or advanced oxidation processes [9] have been the subject of a great number of studies for the treatment of reactive dye containing wastewaters. Nevertheless, the costs of these processes are relatively high or they might not be able to achieve satisfactory color removal. As an alternative, membrane technologies, including reverse osmosis (RO), nanofiltration (NF) and ultrafiltration (UF), have been successfully used to decolorize textile wastewater and have proven to save costs and water consumptions by water recycling [10,11]. Within these technologies, ceramic membranes provide better thermal, chemical and mechanical properties than polymeric ones [12], which made them more resistant and suitable for severe chemical environments [13]. In this way ceramic membranes are taking advantage and gaining popularity over polymeric ones [14]. These intrinsic characteristics fit perfectly with the nature of textile effluents and, in particular, dye-bath effluents, characterized by high temperatures and alkaline conditions [15]. Furthermore, the characteristics of the ceramic membranes also make possible more aggressive cleaning conditions, which allow extended service lifetimes [16].

Membrane fouling, however, is one of the main drawbacks of membrane technologies, since it causes permeate flux decline and changes in selectivity. By that, the overall productivity of the process decreases. Membrane performance is affected by operating conditions such as transmembrane pressure (TMP) and cross-flow velocity (CFV) [17] and by feed characteristics. An important part of

* Corresponding author. Tel.: +34 96 3879633; fax: +34 96 3877639.
E-mail address: elalde1@txp.upv.es (E. Alventosa-deLara).

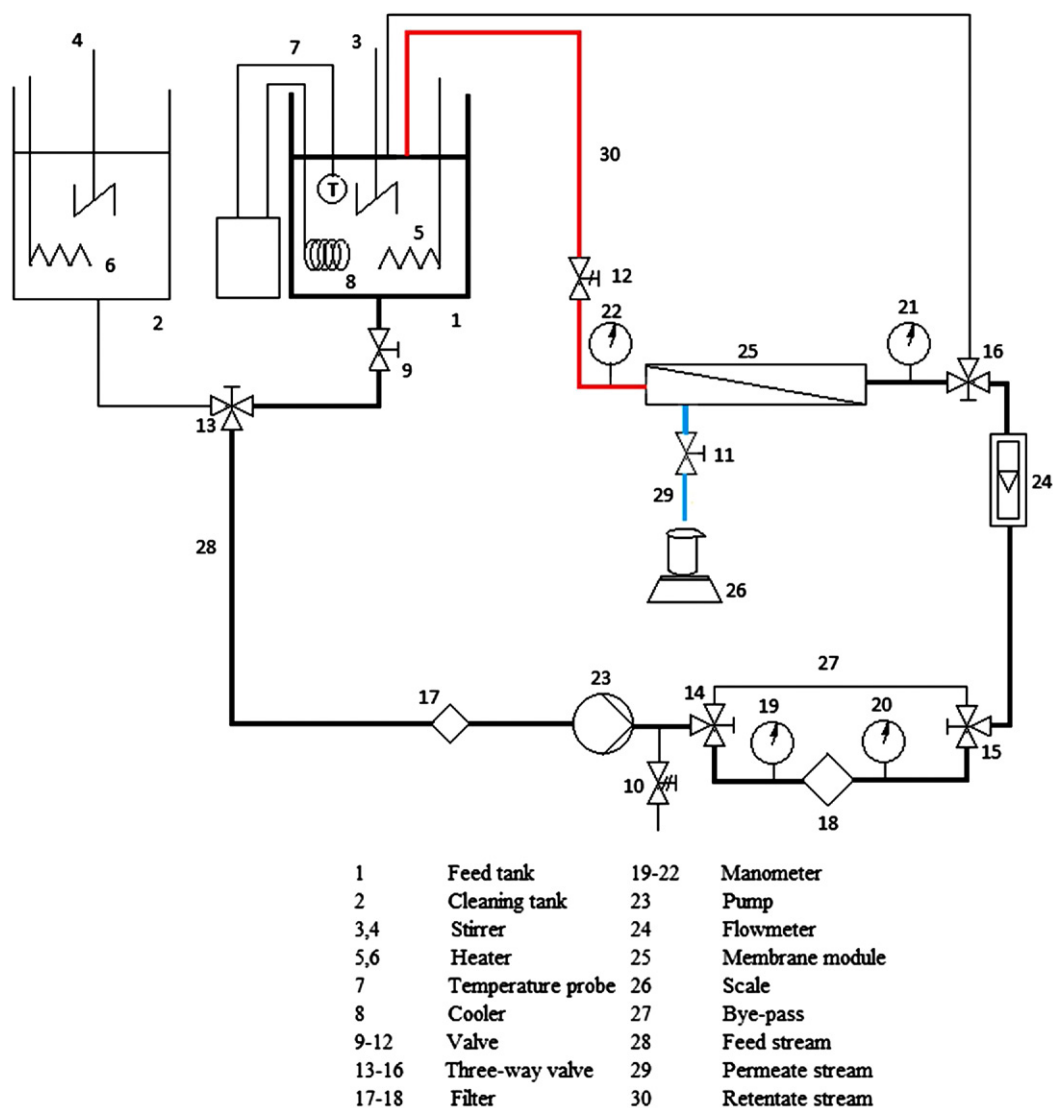


Fig. 1. Scheme of the UF experimental set-up.

the pilot-scale studies is therefore to investigate the factors affecting membrane fouling since if they are known, this phenomenon can be controlled and the optimal operating conditions can be chosen to improve membrane performance. In order to determine the optimal operating conditions, methods such as response surface methodology (RSM) are available. RSM is a set of mathematical and statistical tools used for modeling and analyzing complex processes where a variable response is affected by several factors which can interact among them. When more than a factor is varied in a process it is possible to identify the first and higher order influences of the factors on the response variable. Moreover, RSM is able to predict the interaction effects among the considered factors. In RSM all factors are varied simultaneously and therefore all the conjugated effects are taken into account. The response model can be used for the optimization of the process. RSM has been widely used for the optimization of various processes in wastewater treatment, biotechnology and food industry, among others [18–20]. Scarce literature studying RSM applied to UF processes was found [20,21].

In the present study, an UF multichannel ceramic membrane was used in order to decolorize Reactive Black 5 solutions, determining the effectiveness of the filtration treatments by the evaluation of the rejection coefficients. The aim of the work was to study the impact of operating parameters (TMP and CFV) and

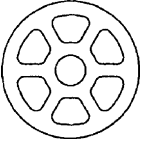
feed characteristics (dye concentration) on the permeate flux and dye rejection. Subsequently RSM was used in order to determine the optimal operating conditions leading to the best membrane performance.

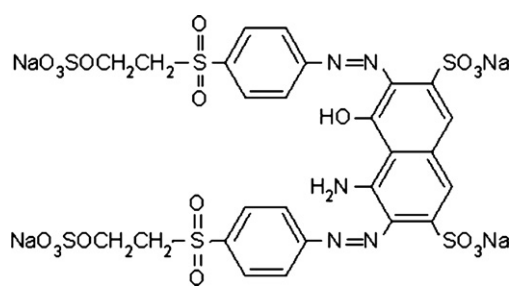
2. Materials and methods

2.1. Experimental set-up

All the tests performed in this study were carried out in an UF pilot plant whose diagram is shown in Fig. 1. The main parts of the installation were a feed tank and a cleaning tank (both including a stirrer fixed at 3000 rpm), which contained the dye solution and the cleaning solution, respectively; a temperature regulating system, which regulated the temperature of the solution in the feed tank; a variable speed pump which allowed the cross-flow velocity to be controlled; the membrane module, with two manometers located at each side of it in order to measure the pressure drop across the module and the valve after the membrane module, which was adjusted to obtain the desired operating TMP. Besides, a 100 μm metallic filter and a 25 μm filter (NW18 Cintropur®) were situated upstream and downstream of the pump, respectively. Both retentate and permeate streams were recirculated to the feed tank and

Table 1
Membrane specifications.

Item	Description
Membrane	INSIDE CÉRAM®
	
Manufacturer	Tami Industries (France)
Type	Tubular
Active layer	ZrO ₂ -TiO ₂
Support material	Titanium
Molecular Weight Cut Off (MWCO)	150 kDa
Deionized water permeability	145.4 L/(m ² h bar)
Length	250 mm
Diameter	10 mm
Number of channels	7
Channel hydraulic diameter	2 mm
Effective filtration area	132 cm ²
Maximum operating temperature	95 °C
Maximum operating pressure	10 bar
pH range	0–14

**Fig. 2.** Molecular structure of Reactive Black 5.

the permeate flux was gravimetrically measured with a scale (0.01 g accuracy).

2.2. Membrane module

An INSIDE CÉRAM® (Tami Industries) multichannel tubular ceramic membrane was used to filter the colored solutions. The specifications of the membrane are given in Table 1.

2.3. Experimental feed solution

The dye used in this study to prepare the colored feed solution was C.I. Reactive Black 5, purchased from Sigma–Aldrich (Germany). Reactive Black 5 is a four valent sodium salt having two sulfonate groups and two sulfatoethylsulfon groups with negative charges within an aqueous solution. It has a molecular weight of 991.82 g/mol and its molecular structure is presented in Fig. 2. The feed solution was prepared by dissolving dye in deionized water until the required concentration was reached. UF experiments were performed at two different dye concentrations: 50 and 500 mg/L. Some characteristics of dye solutions are given in Table 2.

Table 2
Dye solutions characteristics.

Dye concentration	50 mg/L	500 mg/L
pH	6.5	6.81
Conductivity	44.35 μS/cm	388 μS/cm

2.4. Analytical measurements

Feed and permeate concentrations of RB5 were measured using an UV–visible spectrophotometer (Hewlett–Packard 8453) at the wavelength at which maximum absorbance occurred (592 nm). The dye rejection coefficient (R) was calculated as a percentage according to the following equation:

$$R(\%) = \left(1 - \frac{C_p}{C_f}\right) 100 \quad (1)$$

where C_p is the permeate dye concentration and C_f the feed dye concentration.

The permeate flux (J_p) was calculated as follows:

$$J_p = \frac{V}{tA} \quad (2)$$

where V is the volume of water or solution collected from the permeate stream, t stands for sampling time, and A denotes the membrane filtration area.

2.5. Cross-flow filtration

2.5.1. Membrane characterization

The water membrane permeability was determined by measuring the permeate flux of deionized water at different TMP (0.5, 1, 2, 3 and 4 bar). The CFV was set to 3 m/s and the temperature was maintained at 25 °C, as this was the temperature used in the UF experiments of dye solution. The initial water membrane permeability determined was 145.4 L/(m² h bar).

2.5.2. UF of dye solution

In order to investigate the influence of the operating conditions on the membrane performance, UF tests were carried out at four different TMP (1, 2, 3 and 4 bar) and three different CFV (1, 2 and 3 m/s). All the experiments were performed at a constant temperature of 25 °C. Both retentate and permeate streams were recirculated into the feed tank to maintain a constant concentration filtration mode. Moreover, two dye concentrations (50 and 500 mg/L) were tested to observe the effect of the feed concentration. The experiments were long enough to reach the steady-state conditions (after 7–9 h from the beginning of the run). The permeate flux was monitored throughout the UF experiments and samples from both the feed tank and permeate stream were collected at the beginning of the run and subsequently every hour in order to analyze them. Membrane permeability was checked before and after every experiment.

2.6. Membrane cleaning procedure

After each UF run with dye solution, the membrane was subjected to a cleaning cycle which included in the first place a rinse with deionized water at 25 °C (15 min). Next, an alkaline cleaning with aqueous NaOH solution (pH 13) at 60 °C (1 h) took place. Finally, the membrane was rinsed with deionized water until neutrality. The cleaning procedure after runs with feed concentration of 500 mg/L included an additional step since alkaline cleaning was not enough to recover the initial permeability. It consisted in an acid cleaning step with aqueous citric acid solution (pH 2) at 40 °C (1 h), followed by rinsing with deionized water until neutrality was reached. All the cleaning steps, including rinses, were conducted at a CFV of 3 m/s and no pressure was applied. Once the membrane was cleaned, the water permeability was checked following the procedure described in Section 2.5.1. The mentioned cleaning process allowed initial flux recoveries higher than 90%.

Table 3
Experimental design and results for the runs with dye concentration of 50 mg/L.

Run	Factors		Response variables	
	TMP (bar)	CFV (m/s)	J_p (L/(m ² h))	R (%)
1	1	2	160.46	87.4
2	4	2	242.09	91.5
3	2	1	180.14	81.0
4	2	3	215.22	90.4
5	2	2	212.94	95.5
6	2	2	208.59	95.1
7	1	1	107.31	83.1
8	4	1	222.76	88.2
9	1	3	165.98	87.4
10	4	3	265.06	93.0
11	3	1	203.61	79.8
12	3	2	229.03	94.0
13	3	3	266.81	91.8

2.7. Statistical procedures

As reported by Figueroa et al. [20], the operating parameters values which achieve desired characteristics for more than one response variable simultaneously can be determined by means of the Multiple Response Optimization (MRO). To use this procedure, regression models had first to be constructed for each response separately by means of response surface methodology. The response variables were fitted by a second-order model in the form of a quadratic polynomial equation:

$$Y = b_0 + \sum_{i=1}^n b_i X_i + \sum_{i=1}^n b_{ii} X_i^2 + \sum_{i=1}^{n-1} \sum_{j=i+1}^n b_{ij} X_i X_j \quad (3)$$

where Y is the response variable, X_i and X_j the input factors, n the number of factors, b_0 the constant coefficient, b_i the linear coefficients, b_{ii} the quadratic coefficients and b_{ij} the interaction coefficients. The statistical analysis was performed for the two different dye concentrations tested individually, using Statgraphics Centurion XVI[®]. The factors studied were TMP and CFV and the response variables were permeate flux and dye rejection at steady-state conditions. The experiments were performed according to the multi-level experimental designs shown in Tables 3 and 4.

3. Results and discussion

3.1. Influence of operating conditions on permeate flux

3.1.1. Effect of TMP

Fig. 3 illustrates permeate flux (J_p) as a function of TMP for the three CFV studied and a dye concentration of 50 mg/L at the initial

Table 4
Experimental design and results for the runs with dye concentration of 500 mg/L.

Run	Factors		Response variables	
	TMP (bar)	CFV (m/s)	J_p (L/(m ² h))	R (%)
1	1	2	97.94	88.5
2	4	2	212.94	24.0
3	2	1	84.80	72.6
4	2	3	187.46	67.7
5	2	2	185.56	86.4
6	2	2	180.30	85.0
7	1	1	86.72	54.3
8	4	1	76.50	83.2
9	1	3	104.67	88.8
10	4	3	166.96	87.3
11	3	1	84.34	80.2
12	3	2	211.02	70.2
13	3	3	178.47	75.2

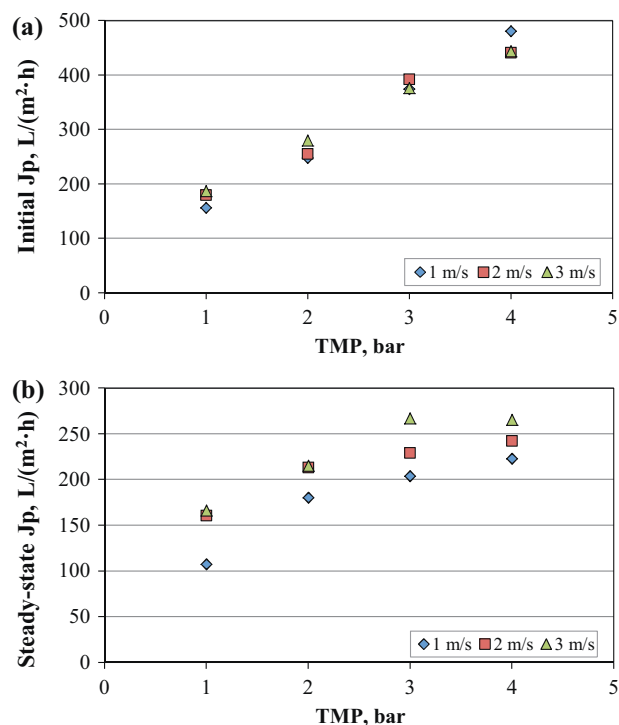


Fig. 3. Effect of TMP on permeate flux at different CFV and dye concentration of 50 mg/L. (a) Initial time, (b) steady-state conditions.

time (a) and at steady-state conditions (b). The steady-state permeate flux value was calculated as the arithmetical average of all the permeate flux measurements in the period between 1 and 2 h before the end of the run.

J_p values at steady-state conditions were lower than J_p initial values under any operating condition (Fig. 3), which indicates that there was a decrease of permeate flux during the experiments. As reported, permeate flux decline is a consequence of membrane fouling and might be due to several factors such as adsorption of dye molecules onto the membrane surface and into the pores, concentration polarization and cake layer formation [22]. The differences between initial and steady-state J_p values were more pronounced at higher TMP (at a fixed CFV of 2 m/s, the flux reduction at 1 bar was 10.4% while at 4 bar was much higher, 45.1%), probably because under these conditions the convection of particles toward the membrane surface is enhanced [23] and thus, dye molecules are more easily deposited onto the membrane surface or into the pores, increasing membrane fouling and leading to a major decrease of permeate flux.

Initially, permeate flux increased with an increase in operating pressure nearly corresponding to a linear equation (Fig. 3a), as expected, since TMP is the driving force of the UF process. Nevertheless, at steady-state conditions (Fig. 3b), when membrane fouling was likely to have occurred as a consequence of the different mechanisms previously stated, the trend was slightly different. For instance, at a fixed CFV of 2 m/s, permeate flux increased by 32.7% as TMP was changed from 1 to 2 bar. By further increasing operating pressure, less significant improvement in steady-state permeate flux was obtained. This was observed at any CFV tested. Moreover, it is worth noting that at the highest CFV, at TMP higher than 3 bar, permeate flux was independent of TMP. This could be attributed to the accumulation of solute particles near the membrane surface and the formation of a cake layer [24]. Steady-state in cross-flow membrane filtration is reached when the solute flux driven toward the membrane by convection is compensated by the back transport of the solute away from the membrane [25]. In this way, this

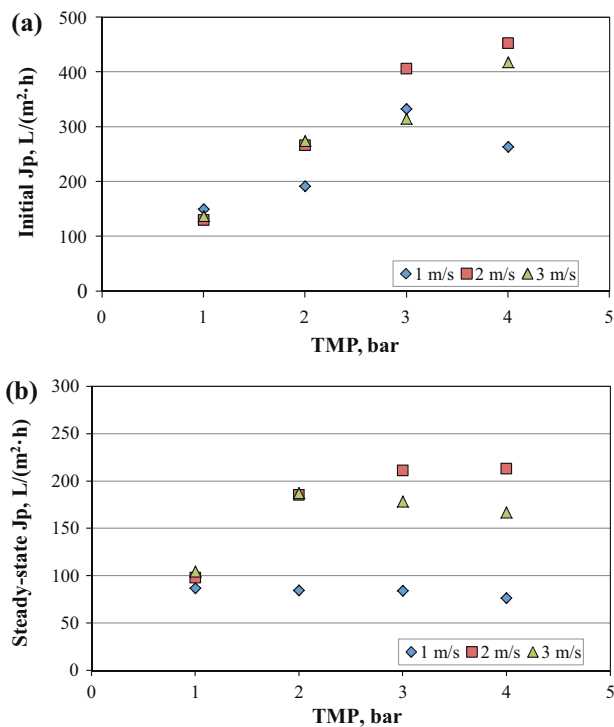


Fig. 4. Effect of TMP on permeate flux at different CFV and dye concentration of 500 mg/L. (a) Initial time, (b) steady-state conditions.

filtration stage is characterized by a constant thickness of the cake layer. When feed pressure increases, a thicker and more compacted cake layer is obtained at the equilibrium state. By that, both the driving force of the filtration process and the filtration resistance are increasing. When these opposed effects are compensating each other, steady-state permeate flux is independent of TMP [26], and the process becomes mass transfer-controlled.

Regarding the experiments with fixed dye concentration of 500 mg/L (Fig. 4), the differences between initial (a) and steady-state behavior (b) were more accused than in the case of lower feed concentration. As it occurred at tests with dye concentration of 50 mg/L, at initial time permeate flux increased, almost linearly, as TMP rose. In this case, however, at the lowest CFV, permeate flux decreased as TMP increased from 3 to 4 bar, probably due to the fact that such a low CFV might not be able to produce adequate turbulence to counteract the effect of higher feed concentration and higher TMP. In this way, more dye molecules could easily approximate to the membrane surface causing membrane fouling in the initial moments, which could indicate pore blocking [27] and resulting in a J_p lower than expected.

Furthermore, the previously commented phenomenon of cake layer formation and compaction was even more significant at the experiments with higher feed concentration (Fig. 4b). At the lowest CFV tested (1 m/s), the permeate flux was independent of TMP and the process was mass transfer-controlled. At CFV of 2 and 3 m/s permeate flux increased with TMP to represent an improvement in steady-state permeate flux of 89.5% and 79.1% respectively at a corresponding TMP increase from 1 to 2 bar. However, at pressures higher than 2 bar slight or no further increase of permeate flux was observed. In fact, at 3 m/s the flux rather started to decrease. This fact may be attributed to the increasing compaction of the surface deposit on the membrane surface, to counteract the effect of higher TMP values [28]. A more compacted cake layer results in a greater filtration resistance, leading to a decrease in steady-state permeate flux. Similar results are reported by Waeger et al. [29]

using ceramic ultrafiltration membranes for particle removal from anaerobic digester effluent.

3.1.2. Effect of CFV

The results obtained during experiments with dye concentration of 50 mg/L showed that permeate flux decline from the beginning of the run to the steady-state condition was lower at higher CFV (Fig. 3). In fact, as an example, for a fixed TMP of 4 bar, permeate flux decreased by 53.6% from its initial value when operating CFV was set at 1 m/s, whereas it decreased by 45.1% and 40.2% at CFV of 2 and 3 m/s, respectively. Lower permeate flux decline as CFV increases is a consequence of the reduction of membrane fouling and concentration polarization under higher CFV. By increasing CFV a greater turbulence is created at the membrane interface, which prevents particle deposition and even removes some of the dye molecules accumulated in the surface [30]. Owing to this fact, concentration polarization is reduced and the deposit layer becomes thinner, which results in a lower filtration resistance and thus, a higher permeate flux.

As it can be seen from Fig. 3b, an increase in CFV from 1 to 2 m/s leads to an increase in steady-state permeate flux ranging from 8.7% to 49.5%, depending on operating pressure. Nevertheless, by further increasing CFV, slight improvements are observed (1.1–16.5%).

It is worth noting that despite having great influence on steady-state permeate flux, very slight effect of CFV on initial J_p was observed at the runs with 50 mg/L (Fig. 3a), since the measured J_p values were similar. However, the influence of CFV can be noticed under certain conditions even at the beginning of the run with high dye concentration (Fig. 4a). The observed differences among the tested CFV are more evident at TMP greater than 1 bar. In this case, generally the lowest initial J_p values were obtained for the lowest CFV tested (1 m/s), which might be attributed to the inadequate turbulence produced at low CFV. Consequently, fouling cannot be effectively combated, leading to lower values of J_p . At steady-state conditions (Fig. 4b), as it occurred at low dye concentration, an increase in flux values by increasing CFV was observed, due to the decrease in dye deposition and concentration polarization. The steady-state permeate flux increased significantly when CFV was increased from 1 to 2 m/s. However, at TMP beyond 2 bar the permeate flux declined at a CFV of 3 m/s. This finding might be explained because, under these conditions, the permeate flux was limited by the dense structure of the deposited fouling layer. As reported by Petrov and Stoychev [31], dye aggregation is possible at high concentrations in the solution and by that, greater particles are formed. At high CFV, the greatest particles are removed due to the turbulence created, allowing the smaller particles to approximate to the membrane surface. In this way, the stratification of the particles according to their size is promoted and a more compact cake layer is formed, resulting in a greater filtration resistance and thus, a permeate flux decline. The counterproductive effect of CFV occurs at high TMP when the tangential forces caused by CFV are lower than the driving force of TMP which approximates the particles to the membrane surface. Similar trends have been observed in previous studies with ceramic ultrafiltration membranes for the filtration of seawater [28] and polyethylene glycol [21].

3.1.3. Effect of feed concentration

As expected, flux decline was greater at higher concentration since as feed concentration increases membrane fouling is more severe. As an example, at a fixed CFV of 2 m/s and dye concentration of 50 mg/L, permeate flux decreased from initial time until steady-state conditions a percentage ranging from 10.4% to 45.1%, depending on TMP. At experiments with higher concentration, instead, it decreased by 24.6–53%. An increase in dye adsorption on the membrane surface and concentration polarization might be the responsible factors for this observation [32,33]. The influence

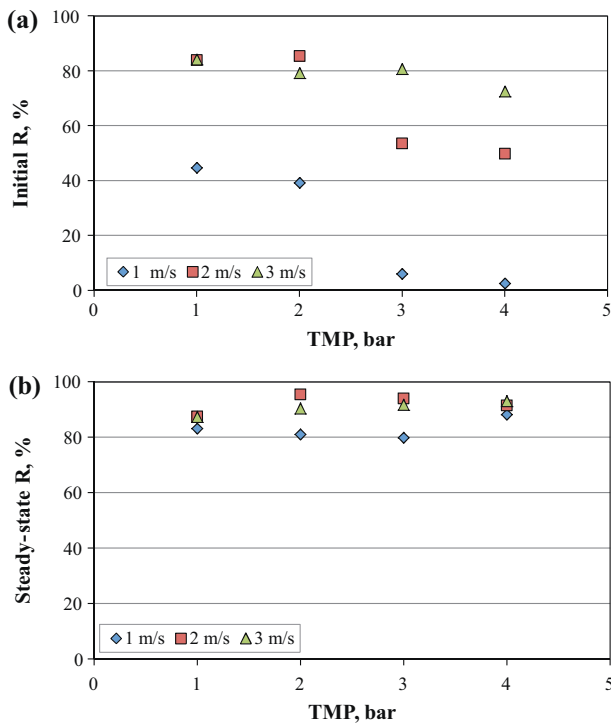


Fig. 5. Effect of TMP on dye rejection coefficient at different CFV and dye concentration of 50 mg/L. (a) Initial time, (b) steady-state conditions.

of feed concentration was more noticeable at steady-state conditions, where J_p values were lower at higher dye concentration. Furthermore, not only J_p values were different depending on feed concentration but also the influence of operating parameters (TMP and CFV) was different according to the concentration used, as stated in Sections 3.1.1 and 3.1.2.

3.2. Influence of operating conditions on dye rejection

Fig. 5 depicts the obtained percentage rejections of RB5 with TMP for the three tested CFV at the initial time (a) and once the steady-state behavior was reached (b) when the dye concentration is 50 mg/L. Due to the low molecular weight of the dye in relation to the MWCO of the tested membrane, the rapid internal fouling due to dye adsorption into the membrane pores is likely to occur. This process is assumed to be the main responsible for the high obtained rejections in the initial minutes of filtration. This adsorption phenomena was also reported in previous studies with dye particles and ceramic membranes [34].

Evident differences between R values at the various CFV tested were observed at the initial time (Fig. 5a), where higher percentage removals were obtained for the highest CFV (72.5–84.1%) while at 1 m/s the R values measured were lower (2.6–44.7%). The higher shear forces induced by the flow velocity over the membrane surface enhance back diffusion of solutes into the bulk solution, counteracting the convective solute flux caused by the imposed driving force (TMP), as well as reducing the concentration polarization layer [35]. In this way, a higher number of dye particles are maintained away from pass through the membrane, thus involving higher percentage of dye removal. On the other hand, for the lowest CFV, the lift forces of the particles are lower. Therefore, the convective forces overcome the shear induced forces and allow a higher number of dye molecules accumulating near the membrane surface and pass through its pores, resulting in a lower retention coefficients. This behavior was corroborated when the applied pressure was increased. Once the applied pressure was increased beyond

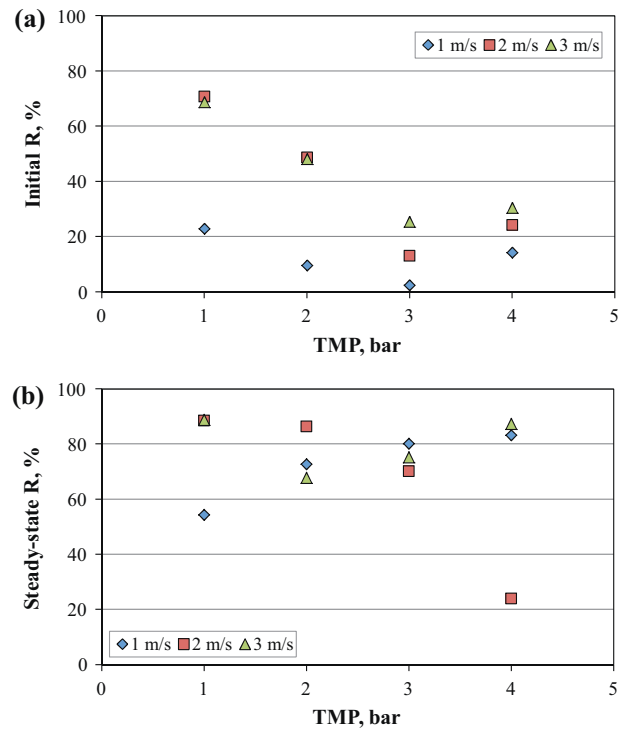


Fig. 6. Effect of TMP on dye rejection coefficient at different CFV and dye concentration of 500 mg/L. (a) Initial time, (b) steady-state conditions.

2 bar, the removal efficiency kept similar values at 3 m/s. However, for lower CFV, the effect exerted by the applied pressure was more noticeable causing more particles pass through the membrane and, therefore, reducing removal efficiency.

Once the steady-state was reached, the differences between R values were not so pronounced (Fig. 5b). In this way, similar results were obtained for the different operating conditions tested, with removals between 79.8% and 95.5%. Similarly to the initial time, the lowest rejection percentages corresponded to the lowest tested CFV. However in this case the highest R values were obtained for CFV of 2 m/s. These considerably satisfactory results highlighted the suitability of this technology in the treatment of colored effluents. The increase in the TMP entails an increase in the number of dye particles transported toward the membrane surface, which may allow the formation of aggregates that increase in size rapidly [36]. The accumulation of these aggregates during the run and the formation of the polarization layer may lead to the formation of a cake layer onto the membrane surface, once the polarization layer has been formed, that controls the filtration process. The formation of adsorbed layers onto the membrane surface was also observed by Bernat et al. in the treatment of iron (III) with ceramic membranes [37].

Regarding the experiments with higher dye concentration Fig. 6 illustrates the rejection coefficients with TMP at the three tested velocities for the 500 mg/L dye solutions at the initial time (a) and for the steady-state conditions (b). It is clear from the figure that, initially (Fig. 6a), process performance in terms of dye rejection diminished either when CFV was reduced or when TMP increased. As explained above, the higher CFV entails higher shear forces and turbulence over the membrane surface sweeping part of the particles and returning them back to the bulk solution [30]. Consequently, dye rejection is improved. On the other hand, the increase in dye concentration increases the possibility of particles passing throughout the membrane. This effect is enhanced by the increase in the driving forces, which increase the convective flow of dye particles toward the membrane surface, allowing their accumulation

and increasing the proportion of dye molecules passing through the membrane. It is highlighted that an increase in TMP beyond 3 bar resulted in a change in the mentioned trend, with an increase in the dye rejection. This behavior might be attributed to the rapid pore blocking due to the high driving force and high dye concentration. In this case, the rapid pore blockage may hinder the pass of dye molecules to some extent increasing slightly the rejection coefficients. Likewise, Lin et al. observed that rapid membrane fouling occurred mainly due to inner pore adsorption and blockage in a loose UF membrane [38].

When the steady-state was reached, the behavior did not show a clear trend (Fig. 6b). In this way, for the lowest tested CFV an increase in TMP entailed higher dye rejection. This effect is associated to the accumulation of a higher number of dye particles near the membrane surface, which enhances the increase of the polarization layer thickness. At the same time, the higher applied pressure may involve the compression of the formed layer leading to a denser structure [39]. The opposite effect was observed when the CFV was raised to 2 m/s, since an increase in TMP entailed lower rejection percentages. The higher shear forces allow the back diffusion of some dye particles to the bulk solution, reducing the layer thickness. This fact combined with an increase in the convective drag forces would enhance the permeation through the membrane and hence, the rejection coefficients would be reduced [40]. In the case of the highest tested CFV a different behavior was observed. Although an initial decrease in dye retention was observed with TMP, beyond 2 bar, the dye retention slightly increased with similar percentages obtained for the lowest applied pressure. These effects are attributed to the influence of counteracting effects produced by the different forces involved in the process like the shear diffusion, electroviscous effects, convective forces and electrostatic forces.

Regarding the feed concentration, it can be observed that higher dye concentration entailed lower dye rejection. In particular, dye rejection for the less concentrated solution (50 mg/L) ranged between 79.8 and 95.5%, with an average rejection of 88.6%, depending on the operating conditions. On the other hand, when dye concentration was increased to 500 mg/L, the loss in removal efficiency was significant with a final average rejection around 73.2%.

3.3. Statistical analysis

The effects of the factors and their interactions on the response variables were obtained by means of analysis of variance (ANOVA). The Pareto chart resulting from the analysis of the permeate flux for the experiments with dye concentration of 50 mg/L is shown in Fig. 7a. The bars crossing the vertical line indicate that the corresponding effect is significant at a confidence level of 95%. In addition, the sign of the effect indicates if it produces an increase (+) or a decrease (–) of the variable response. The quadratic regression equation obtained for the permeate flux including only the statistically significant coefficients was the following:

$$J_p = 12.9901 + 94.9486\text{TMP} + 24.9064\text{CFV} - 12.4979\text{TMP}^2 \quad (4)$$

The regression coefficient R^2 , which indicates the variability in permeate flux explained by the model as fitted, was 96.28% and the Standard Error was 3.07309. The p -value for lack-of-fit was greater than 5% ($p=0.2216$), thus the model appears to be adequate for the observed data at a 95% confidence level. Residual analysis showed that since the p -value of Durbin–Watson statistic was greater than 5% ($p=0.7781$) and the Lag 1 Residual Autocorrelation was nearly 0 (-0.364557), there was no indication of serial autocorrelation in the residuals at the 5% significance level.

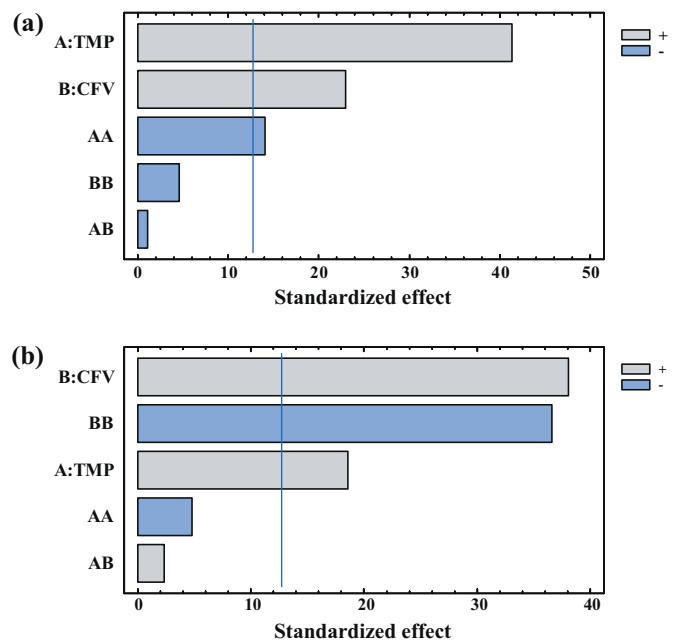


Fig. 7. Pareto charts from the analysis of (a) permeate flux and (b) dye rejection at dye concentration of 50 mg/L.

Fig. 7b shows the Pareto chart obtained from the analysis of dye rejection for runs with 50 mg/L. Eq. (5) was the quadratic regression equation obtained for the dye rejection including only the statistically significant coefficients:

$$R = 57.8482 + 1.33941\text{TMP} + 27.839\text{CFV} - 6.00819\text{CFV}^2 \quad (5)$$

The R^2 statistic indicated that 76.6% of the variability in dye rejection was explained by the model as fitted. The Standard Error was 0.282843 and the p -value for lack-of-fit was greater than 5% ($p=0.0699$). Therefore, the model seems adequate for the observed data at a confidence level of 95%. Additionally, the p -value of Durbin–Watson statistic ($p=0.0615$) and the Lag 1 Residual Autocorrelation (0.317347) showed that there was no indication of serial autocorrelation in the residuals.

In the same way, the statistical analysis was performed for the runs with dye concentration of 500 mg/L. The results of the analysis of J_p are shown in the Pareto chart in Fig. 8a. Once the no statistically significant coefficients were removed, the equation describing the effect of the process variables on J_p was the following:

$$J_p = -239.744 + 93.7323\text{TMP} + 258.101\text{CFV} - 15.2814\text{TMP}^2 - 54.9876\text{CFV}^2 \quad (6)$$

In this case, the R^2 statistic and the Standard Error were 83.43% and 3.7215 respectively. The p -value for lack-of-fit ($p=0.0988$) indicated that the model appeared to be adequate for the data at a 95% confidence level. The obtained results for the p -value of Durbin–Watson, which was greater than 5% ($p=0.7596$) and the Lag 1 Residual Autocorrelation, which was around 0 (-0.348344), showed no indication of serial autocorrelation in the residuals at the 5% significance level.

Finally, Fig. 8b presents the Pareto chart resulting from the analysis of dye rejection for runs with 500 mg/L. The R^2 of the model obtained after removing the no statistically significant coefficients was 11.61% and the p -value for lack-of-fit was lower than 5% ($p=0.0387$), which indicated that the model was not adequate to represent the experimental data. Therefore it was decided do not include it in the study.

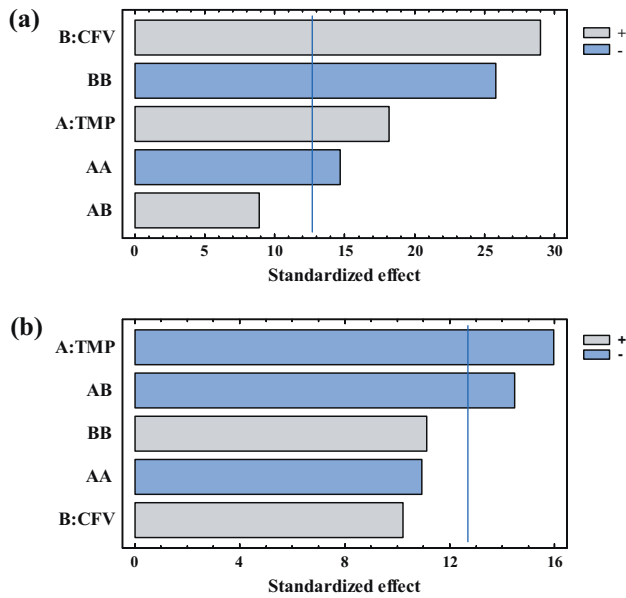


Fig. 8. Pareto charts from the analysis of (a) permeate flux and (b) dye rejection at dye concentration of 500 mg/L.

3.4. Optimization of operating conditions

An optimal membrane performance ensures maximum permeate flux while having maximum solute rejection [41] and it is highly affected by operating conditions such as TMP and CFV. Therefore, the goal of the optimization in the present study was to find operating conditions (TMP and CFV) which maximized both the permeate flux and dye rejection at steady-state conditions simultaneously. Once the fitted models were obtained, Multiple Response Optimization was used to determine settings of the experimental factors which achieved optimal operating conditions. As reported before, owing to the low accuracy of the model for the dye rejection for runs with 500 mg/L feed concentration, it was not taken into account for the study. Therefore, MRO was performed for the runs with feed concentration of 50 mg/L. This was done by using the desirability function (DF) method. In this method, the statistical software retrieves information from each of the previously analyzed designs in order to construct a DF based on values of the response variables, which is then maximized. In order to combine multiple responses into a single function that can be maximized, a desirability function, $d(y)$, is first defined for each response, expressing the desirability of a response value equal to y on a scale of 0–1. If a response variable is to be maximized, $d(y)$ is defined by:

$$d = \begin{cases} 0 & \hat{y} < \text{low} \\ \left(\frac{\hat{y} - \text{low}}{\text{high} - \text{low}} \right)^s & \text{low} \leq \hat{y} \leq \text{high} \\ 1 & \hat{y} > \text{high} \end{cases} \quad (7)$$

where \hat{y} is the predicted value of the response variable, low is a value below which the response is completely unacceptable, and high is a value above which the desirability is at its maximum. The parameter s defines the shape of the function. By default, the DF are linear. To combine the desirabilities of all responses, a single composite function, D , is created. If all the response variables are considered to be equally important, then D is the geometric mean of the separate desirabilities. The minimum and maximum limits used for J_p and R were 107.31 L/(m² h) ($d=0$), 266.81 L/(m² h) ($d=1$), 79.8% ($d=0$) and 95.5% ($d=1$) respectively, which corresponded to the minimum and maximum values obtained experimentally. The surface plot corresponding to the resulting desirability function

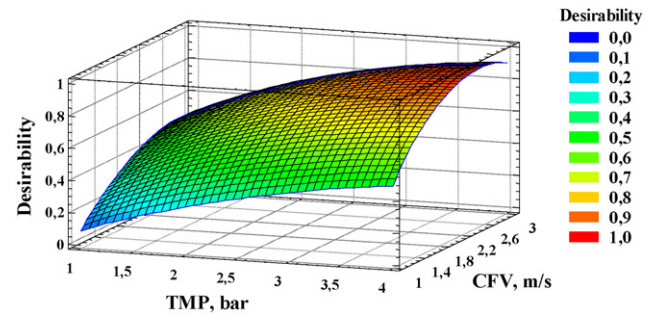


Fig. 9. Surface plot for the overall desirability function at dye concentration of 50 mg/L.

Table 5

Optimization results for the runs with dye concentration of 50 mg/L.

Optimized factors	TMP (bar)	4
	CFV (m/s)	2.53
Overall desirability		0.96
Predicted	J_p (L/(m ² h))	255.86
response variables	R (%)	95.2

D is shown in Fig. 9. The values of the operating conditions that maximize the overall desirability function and the corresponding response variable values predicted are shown in Table 5. At these conditions the overall desirability is predicted to equal almost 0.96. The optimal value of TMP corresponded to the highest TMP tested while optimal CFV was slightly lower than the highest value tested. Under optimal operating conditions, the predicted values of J_p and R were close to the maximum values obtained experimentally.

4. Conclusions

The performance of an ultrafiltration ceramic membrane during the removal of Reactive Black 5 was evaluated by modifying the operating conditions (TMP and CFV) and the feed dye concentration. The influence of these parameters on both the permeate flux and dye rejection at initial and steady-state conditions was discussed. The experimental results revealed that flux decline was more pronounced at higher TMP, lower CFV and higher feed concentration. There was a positive influence of TMP on permeate flux, which initially increased almost linearly with TMP. Nevertheless, at steady-state conditions there was a value of TMP beyond which permeate flux did not increase with the applied TMP. This value was different depending on CFV and feed concentration.

CFV exerted a positive influence on permeate flux as well, although this influence diminished as CFV was higher. However, there was a limit on this positive effect since at runs with high dye concentration an increase in CFV from 2 to 3 m/s led to a decline on steady-state permeate flux.

Dye rejection coefficients were used to evaluate the effectiveness of UF treatment on the removal of dye. For the runs at 50 mg/L, the results were quite similar once the steady-state behavior was reached, although the lowest rejection percentages corresponded to the lowest tested CFV. The dye rejection observed when the dye concentration was 500 mg/L showed no clear trend and was dependent on the different forces involved in the filtration process. Regardless of the tested conditions, a decrease in rejection performance was observed when dye concentration increased. Nevertheless, the obtained results showed a significant dye removal by means of the ultrafiltration process with rejection coefficients higher than 79.8% and an average rejection of 88.6% for the lowest tested concentration and around 73.2% for the 500 mg/L runs.

Finally, the response surface methodology proved to be a useful tool to optimize the process, making it possible to establish the best operating conditions leading to the maximum steady-state permeate flux and the highest dye rejection coefficient simultaneously. For the runs with dye concentration of 50 mg/L, the optimal conditions found were 4 bar and 2.53 m/s. Regarding dye concentration of 500 mg/L, the optimal operating conditions could not be determined owing to the low accuracy of the model obtained for dye rejection coefficient.

Acknowledgments

This research has been financially supported by the Spanish Ministerio de Ciencia e Innovación (MICINN) through the project ref. CTM2009-13048. The authors of this work also acknowledge the assistance of the Spanish Ministerio de Educación for the award of a F.P.U. grant (Ref. AP2009-3509).

References

- [1] S. Rosa, M.C. Laranjeira, H.G. Riela, V.T. Fávere, Cross-linked quaternary chitosan as an adsorbent for the removal of the reactive dye from aqueous solutions, *J. Hazard. Mater.* 155 (2008) 253–260.
- [2] S.M. Burkinshaw, O. Kabambe, Attempts to reduce water and chemical usage in the removal of bifunctional reactive dyes from cotton: part 2 bis(vinyl sulfone) aminochlorotriazine/vinyl sulfone and bis(aminochlorotriazine/vinyl sulfone) dyes, *Dyes Pigments* 88 (2011) 220–229.
- [3] A.L. Ahmad, S.W. Puasa, Reactive dyes decolorization from an aqueous solution by combined coagulation/micellar-enhanced ultrafiltration process, *Chem. Eng. J.* 132 (2007) 257–265.
- [4] S. Vajnhandi, A.M.L. Marechal, Case study of the sonochemical decoloration of textile azo dye Reactive Black 5, *J. Hazard. Mater.* 141 (2007) 329–335.
- [5] B. Bonakdarpour, I. Vyrides, D.C. Stuckey, Comparison of the performance of one stage and two stage sequential anaerobic-aerobic biological processes for the treatment of reactive-azo-dye-containing synthetic wastewaters, *Int. Biodeter. Biodegr.* 65 (2011) 591–599.
- [6] Y.S. Al-Degs, M.I. El-Barghouti, A.H. El-Sheikh, G.M. Walker, Effect of solution pH, ionic strength, and temperature on adsorption behavior of reactive dyes on activated carbon, *Dyes Pigments* 77 (2008) 16–23.
- [7] G. Annadurai, L.Y. Ling, J.-F. Lee, Adsorption of reactive dye from an aqueous solution by chitosan: isotherm, kinetic and thermodynamic analysis, *J. Hazard. Mater.* 152 (2008) 337–346.
- [8] I.A. Sengil, M. Özacar, The decolorization of C.I. Reactive Black 5 in aqueous solution by electrocoagulation using sacrificial iron electrodes, *J. Hazard. Mater.* 161 (2009) 1369–1376.
- [9] M.S. Lucas, A.A. Dias, A. Sampaio, C. Amaral, J.A. Peres, Degradation of a textile reactive Azo dye by a combined chemical–biological process: Fenton's reagent-yeast, *Water Res.* 41 (2007) 1103–1109.
- [10] T.-H. Kim, C. Park, S. Kim, Water recycling from desalination and purification process of reactive dye manufacturing industry by combined membrane filtration, *J. Cleaner Prod.* 13 (2005) 779–786.
- [11] R. Han, S. Zhang, D. Xing, X. Jian, Desalination of dye utilizing copoly(phthalazinone biphenyl ether sulfone) ultrafiltration membrane with low molecular weight cut-off, *J. Membr. Sci.* 358 (2010) 1–6.
- [12] I. Jedidi, S. Saïdi, S. Khemakhem, A. Larbot, N. Elloumi-Ammar, A. Fourati, A. Charfi, A.B. Salah, R.B. Amar, Elaboration of new ceramic microfiltration membranes from mineral coal fly ash applied to waste water treatment, *J. Hazard. Mater.* 172 (2009) 152–158.
- [13] S.G. Lehman, L. Liu, Application of ceramic membranes with pre-ozonation for treatment of secondary wastewater effluent, *Water Res.* 43 (2009) 2020–2028.
- [14] R. Pérez-Gálvez, E.M. Guadix, J.-P. Bergé, A. Guadix, Operation and cleaning of ceramic membranes for the filtration of fish press liquor, *J. Membr. Sci.* 384 (2011) 142–148.
- [15] C. Allègre, P. Moulin, M. Maiseu, F. Charbit, Treatment and reuse of reactive dyeing effluents, *J. Membr. Sci.* 269 (2006) 15–34.
- [16] M.C. Almecija, A. Martínez-Ferez, A. Guadix, M.P. Paez, E.M. Guadix, Influence of the cleaning temperature on the permeability of ceramic membranes, *Desalination* 245 (2009) 708–713.
- [17] M.C.V. Vela, S.Á. Blanco, J.L. García, E.B. Rodríguez, Analysis of membrane pore blocking models adapted to crossflow ultrafiltration in the ultrafiltration of PEG, *Chem. Eng. J.* 149 (2009) 232–241.
- [18] J. Landaburu-Aguirre, E. Pongrácz, P. Perämäki, R.L. Keiski, Micellar-enhanced ultrafiltration for the removal of cadmium and zinc: use of response surface methodology to improve understanding of process performance and optimization, *J. Hazard. Mater.* 180 (2010) 524–534.
- [19] N. Aktas, İ.H. Boyacı, M. Mutlu, A. Tanyolac, Optimization of lactose utilization in deproteinated whey by *Kluyveromyces marxianus* using response surface methodology (RSM), *Bioresour. Technol.* 97 (2006) 2252–2259.
- [20] R.A.R. Figueroa, A. Cassano, E. Drioli, Ultrafiltration of orange press liquor: optimization for permeate flux and fouling index by response surface methodology, *Sep. Purif. Technol.* 80 (2011) 1–10.
- [21] M.-C. Martí-Calatayud, M.-C. Vincent-Vela, S. Álvarez-Blanco, J. Lora-García, E. Bergantiños-Rodríguez, Analysis and optimization of the influence of operating conditions in the ultrafiltration of macromolecules using a response surface methodological approach, *Chem. Eng. J.* 156 (2010) 337–346.
- [22] F.J. Benítez, J.L. Acero, F.J. Real, C. García, Removal of phenyl-urea herbicides in ultrapure water by ultrafiltration and nanofiltration processes, *Water Res.* 43 (2009) 267–276.
- [23] R. Das, C. Bhattacharjee, S. Ghosh, Effects of operating parameters and nature of fouling behavior in ultrafiltration of sesame protein hydrolysate, *Desalination* 237 (2009) 268–276.
- [24] Y. He, G. Li, Z. Jiang, H. Wang, J. Zhao, H. Su, Q. Huang, Diafiltration and concentration of Reactive Brilliant Blue KN-R solution by two-stage ultrafiltration process at pilot scale: technical and economic feasibility, *Desalination* 279 (2011) 235–242.
- [25] C. Vincent-Vela, B. Cuartas-Urbe, S. Álvarez-Blanco, J. Lora-García, E. Bergantiños-Rodríguez, Analysis of ultrafiltration processes with dilatant macromolecular solutions by means of dimensionless numbers and hydrodynamic parameters, *Sep. Purif. Technol.* 75 (2010) 332–339.
- [26] S. Buethorn, F. Carstensen, T. Wintgens, T. Melin, D. Volmering, K. Vossenkaul, Permeate flux decline in cross-flow microfiltration at constant pressure, *Desalination* 250 (2010) 985–990.
- [27] M. Simonic, Efficiency of ultrafiltration for the pre-treatment of dye-bath effluents, *Desalination* 245 (2009) 701–707.
- [28] J. Xu, C.-Y. Chang, C. Gao, Performance of a ceramic ultrafiltration membrane system in pretreatment to seawater desalination, *Sep. Purif. Technol.* 75 (2010) 165–173.
- [29] F. Waeger, T. Delhay, W. Fuchs, The use of ceramic microfiltration and ultrafiltration membranes for particle removal from anaerobic digester effluents, *Sep. Purif. Technol.* 73 (2010) 271–278.
- [30] F.J. Benítez, J.L. Acero, A.I. Leal, M. González, The use of ultrafiltration and nanofiltration membranes for the purification of cork processing wastewater, *J. Hazard. Mater.* 162 (2009) 1438–1445.
- [31] S.P. Petrova, P.A. Stoychev, Ultrafiltration purification of waters contaminated with bifunctional reactive dyes, *Desalination* 154 (2003) 247–252.
- [32] I. Koyuncu, Reactive dye removal in dye/salt mixtures by nanofiltration membranes containing vinylsulphone dyes: effects of feed concentration and cross flow velocity, *Desalination* 143 (2002) 243–253.
- [33] S. Chakraborty, M.K. Purkait, S. DasGupta, S. De, J.K. Basu, Nanofiltration of textile plant effluent for color removal and reduction in COD, *Sep. Purif. Technol.* 31 (2003) 141–151.
- [34] K.M. Majewska-Nowak, Application of ceramic membranes for the separation of dye particles, *Desalination* 254 (2010) 185–191.
- [35] A. Cassano, A. Mecchia, E. Drioli, Analyses of hydrodynamic resistances and operating parameters in the ultrafiltration of grape must, *J. Food Eng.* 89 (2008) 171–177.
- [36] P. Aimar, P. Bacchin, Slow colloidal aggregation and membrane fouling, *J. Membr. Sci.* 360 (2010) 70–76.
- [37] X. Bernat, A. Pihlajamäki, A. Fortuny, C. Bengoa, F. Stüber, A. Fabregat, M. Nyström, J. Font, Non-enhanced ultrafiltration of iron(III) with commercial ceramic membranes, *J. Membr. Sci.* 334 (2009) 129–137.
- [38] C.F. Lin, A.Y.-C. Lin, P. Sri Chandana, C.Y. Tsai, Effects of mass retention of dissolved organic matter and membrane pore size on membrane fouling and flux decline, *Water Res.* 43 (2009) 389–394.
- [39] C. Park, Y.H. Lee, S. Lee, S. Hong, Effect of cake layer structure on colloidal fouling in reverse osmosis membranes, *Desalination* 220 (2008) 335–344.
- [40] F.J. Benítez, J.L. Acero, A.I. Leal, Application of microfiltration and ultrafiltration processes to cork processing wastewaters and assessment of the membrane fouling, *Sep. Purif. Technol.* 50 (2006) 354–364.
- [41] S.S. Sablani, M. Goosen, R. Al-Belushi, M. Wilf, Concentration polarization in ultrafiltration and reverse osmosis: a critical review, *Desalination* 141 (2001) 269–289.